Int. J. Electrochem. Sci., 17 **(2022)** Article Number: 220122, doi: 10.20964/2022.01.32

International Journal of
ELECTROCHEMICAL
SCIENCE
www.electrochemsci.org

Elucidation of the stoichiometry of Fe(III) and Fe(II) complexes formed with 2-(5-bromo-2-pyridylazo)-5-diethylaminophenol (5-Br-PADAP). Application to Fe(III) and Fe(II) Electrochemical Determination at Trace Level in Natural Water

Nabiil Auckburally[1,2], *Souheila El Bir*[1], *David Evrard*[1,*], *Brigitte Dustou*[1], *Laure Latapie*[1], *Laurent Boumati*[2], *Christine Roques*[1], *Pierre Gros*[1]

[1] Laboratoire de Génie Chimique, Université de Toulouse, CNRS, INPT, UPS, Toulouse, France
[2] Resonet Services, Zone Artisanale Lafourcade, 32200 Gimont
[*]E-mail: david.evrard@univ-tlse3.fr

Received: 26 September 2021 / *Accepted:* 25 October 2021 / *Published:* 6 December 2021

This work provides some new information on the complexes formed between Fe(III) and Fe(II) with 2-(5-bromo-2-pyridylazo)-5-diethylaminophenol (5-Br-PADAP). The electrochemical behavior of both complexes was studied and their stoichiometry, which was uncertain till now, was definitely clarified as a 1:1 metal:ligand ratio on the basis of both electrochemical and spectrophotochemical data. The stability constants β for both complexes were also determined and found to be in the range 10^5 and 10^4 for Fe(III)/ and Fe(II)/5-Br-PADAP complex, respectively. Using 5-Br-PADAP as a complexing agent, the determination of Fe at trace level in water was achieved by adsorptive differential pulse voltammetry in the range 1 – 10 µM. Under optimized conditions, a sensitivity of 0.0376 and 0.0063 µA $µM^{-1}$ was found for Fe(III) and Fe(II), respectively. Tests on natural water from Canal du Midi were performed, and allowed values of 2.3 µM for Fe(III) and 1.7 µM for Fe(II) to be obtained. The corresponding value for total Fe was slightly lower than that found with ICP-OES measurements (ca. 4.0 vs. 4.5 µM, respectively), suggesting that 5-Br-PADAP is not a complexing agent strong enough to catch Fe cations in the complexes formed with organic matter nor to complex quantitatively free Fe(III) or Fe(II) species.

Keywords: Complex stoichiometry; 5-Br-PADAP complexation; iron speciation; electrochemical sensor; natural water samples

1. INTRODUCTION

Iron (Fe) is one of the most common element, as it is the fourth most abundant component of the Earth's crust [1]. It can be found in the environment in many soil mineral species, rocks and waters [2], and plays an important role in many systems related to environmental, industrial, biological or human

health concerns [3]. Indeed, in healthy individuals, transferrin-bound Fe is used for hemoglobin synthesis in bone marrow, this haemoprotein being essential for the release of oxygen into the tissues to allow aerobic cellular respiration [4]. On the contrary, hyperferritinemia can cause cataract syndrome [5]. The key role of many siderophores able to complex iron during virulence for many bacterial pathogens has been widely demonstrated [6]. Fe is also essential for photosynthesis [7] and has been reported to be a limiting growth nutrient for phytoplankton in open seawaters [8]. It also plays a key role in ruling some biogeochemical cycles that influence the environmental availability of trace elements [9]. For instance, the reductive dissolution of hydrous ferric oxide by specific bacteria has been recently correlated to the presence of unusually high As(III) concentrations in Bangladeshi ground water [10]. Fe concentration may vary from nM or sub-nM in natural areas such as mid-ocean surface waters [11] up to mM in polluted urban areas [12] or acid mine drainage basins [13]. River waters often exhibit Fe concentrations in the µM range [14]. Although neither the World Health Organization nor the European Union has delivered a guideline value for Fe concentration in drinking water, permissible values usually range from 5 to 55 µM since higher concentrations make water become discolored and taste metallic [15]. Thus, the detection and quantification of Fe is of key interest for many research fields. Since Fe can be found as Fe^0, Fe(II) and Fe(III), the determination of total Fe content is insufficient, and its speciation is of primary importance for meaningful analysis [16]. Indeed, thermodynamic and physicochemical properties of Fe species strongly depend on the metal oxidation state [15]. Considering only the most common oxidation states, Fe(II) is much more soluble than Fe(III) in water, but it is readily oxidized in the presence of oxygen [15], whereas Fe(III) forms very strong, thermodynamically stable complexes with numerous organic ligands despite of its low solubility [17].

The numerous techniques used for the determination of Fe concentration and speciation have been recently reviewed [18,19]. These latter include atomic absorption (AAS) or inductively coupled plasma-mass spectrometry (ICP-MS), chemiluminescence and fluorescence. However, a rapid overview of the literature shows that spectrophotometry and electrochemistry are often preferred with respect to this latter concern [15,20], probably because of their low cost and portability. Whatever the chosen technique, a strategy frequently encountered consists in the use of an organic compound that acts as a complexing or chelating agent for Fe, and thus forms a complex the detection of which is favored because it exhibits a strong color or a significant preconcentration effect. Various ligands have been reported in the literature for this purpose, such as naphtol derivatives [21-24], 2,3-dihydroxynaphthalene [25-27], salicylaldoxime [28] or 2-(2-thiazolylazo)-p-cresol [29]. However, the complexation reaction times for these latter compounds have been reported to be quite long [30]. On the contrary, 2-(5-bromo-2-pyridylazo)-5-diethylaminophenol (5-Br-PADAP) has been found to form a chelate with Fe within a relatively short reaction time (ca. 3 min) [31-33]. This is mainly due to its electron-donating azo and hydroxyl groups that provide a high chelating affinity for Fe [30]. Although it has been reported in many papers, the interaction between 5-Br-PADAP and Fe, both in its Fe(III) and Fe(II) forms, is still not well understood yet: in particular, a discrepancy still exists about the actual stoichiometry of the Fe(III)/5-Br-PADAP and Fe(II)/5-Br-PADAP complexes between a 1:1 or 1:2 metal:ligand ratio (Table 1). Indeed, we found only two works in which the determination of the stoichiometry of the Fe(III)/5-Br-PADAP and Fe(II)/5-Br-PADAP complexes has been actually studied [31,34]. In the work by Oszwaldowski and Pikus [34], the metal:ligand ratio has been determined for both Fe(III) and Fe(II) complexes using the

Bent-French method [35]. Both complexes have been found to exhibit a 1:2 ratio. The corresponding stability constants have been also determined and found to be very close: $10^{9.8}$ and 10^{10} for Fe(II) and Fe(III) complexes, respectively. Fu-sheng et al. have also reported a 1:2 stoichiometry and a stability constant $10^{13.3}$ for the Fe(III) complex [36]. On the contrary, in the report by Zhao et Jin [31], electrochemical means have been used for the determination of the stoichiometry, and a 1:1 metal:ligand ratio has been obtained for Fe(III)/5-Br-PADAP. Checking more carefully the electrochemical studies, some other different information appeared: depending on the considered work, 5-Br-PADAP has been found to exhibit two reduction peaks on Hg [31] and only one on glassy carbon and on reduced graphene oxide / gold nanoparticles modified electrodes [33], whereas Ghoneim claimed that it is actually electroinactive on a carbon paste electrode [37]. Zhu et al. did not mention any reduction peak for 5-Br-PADAP although they performed Fe(III) determination in the presence of a large excess of ligand [30].

In this work, we report on a new study which definitely establishes the stoichiometry of the Fe(III)/5-Br-PADAP and Fe(II)/5-Br-PADAP complexes. This latter was determined by both electrochemical and spectrophotometric experiments using different initial metal:ligand ratio. The stability constants β of the complexes were also evaluated and compared to values previously reported in the literature. Considerations on the electrochemical reduction process of both the complex and the free ligand are also provided. These results were used to extend the determination of Fe(II) and Fe(III) in the presence of 5-Br-PADAP to the µM concentration range. Tests in natural water from Canal du Midi were also conducted.

2. EXPERIMENTAL

2.1. Chemicals

All chemicals were of analytical grade and used as received. 2-(5-bromo-2-pyridylazo)-5-diethylaminophenol (5- Br-PADAP) ($C_{15}H_{17}BrN_4O$, 98%), iron(III) chloride hexahydrate ($FeCl_3 \bullet 6 H_2O$, 99%) and iron(II) sulfate heptahydrate ($FeCl_2 \bullet 7 H_2O$, 99%) were purchased from Acros Organics. Sodium acetate (99%) was supplied by Aldrich. Acetic acid (99%) was obtained from Fisher. Absolute ethanol (99%), hydrochloric acid (30%, suprapur grade) and sulfuric acid (95%, Normapure grade) were provided by VWR Chemicals.

5-Br-PADAP was prepared as a 2 mM ethanol solution because of its poor solubility in water. All the other solutions were prepared using ultrapure water (Milli-Q, Millipore, 18.2 MΩ□cm) and deaerated by bubbling Nitrogen during 10 min. A gas stream was maintained over the solutions during experiments.

2.2. Apparatus

All electrochemical experiments were performed at room temperature using a Metrohm µ-Autolab II or a PGStat 128N potentiostat interfaced to a personal computer and controlled with NOVA 2.1.5 software package. A classical three-electrode glass cell was used with a Metrohm platinum rod and a Radiometer saturated calomel electrode (SCE) connected to the cell by a capillary as counter and

reference electrode, respectively. All the potentials are expressed with respect to SCE. Working electrode was a 2-mm diameter gold (Au) rotating disk electrode from Radiometer.

UV-visible measurements were recorded on a Perkin Elmer Lambda 365 spectrophotometer using the UV Express software.

Inductive Coupled Plasma – Optical Emission Spectroscopy (ICP-OES) was performed on a HORIBA Ultima 2 spectrometer using a 1000 µg mL^{-1} Fe standard solution in 4 % HNO_3 from SCP Science.

Organic matter digestion was conducted by UV treatment of natural water using a Medium Pressure UV Lamp Heraeus TQ 150. Samples were irradiated for 10 min.

2.3. Electrode preparation

The Au electrode was carefully polished by a 1 µM and 0.3 µM alumina slurry on a polishing cloth pad for 2 min each. Between each polishing step, the electrode surface was rinsed with Milli-Q water. Finally, the electrode was sonicated for 5 min in a 96% ethanol solution. Prior to measurements, the Au electrode was cleaned electrochemically in a deaerated 0.5 M H_2SO_4 solution by cycling the electrode potential between 0 V and 1.5 V at 100 mV s^{-1} until reproducible voltammograms were obtained.

2.4. Detection procedure

Electrochemical measurements were conducted in a 0.1 M acetate buffer (pH 6) as supporting electrolyte containing 30 µM 5-Br-PADAP. First, a potential of -0.12 V was applied for 6 min under stirring as a preconcentration step. Then a cathodic scan was recorded from -0.20 V to -0.60 V or from -0.11 to 0.70 V using differential pulse voltammetry (DPV) with the following conditions: pulse amplitude = 50 mV; step amplitude = 4 mV; pulse time = 50 ms; scan rate = 8 mV s^{-1}. These latter experimental conditions including the preconcentration step were used for all DPV measurements.

2.5. Water sampling and conditioning

Natural water dedicated to Fe(III) and Fe(II) determination was collected from Canal du Midi, on the campus of the Paul Sabatier University in Toulouse (43° 46’ 34.7002’’ N, 1° 15’ 35.2015’’E). A sample was taken in a pre-cleaned 2L-Teflon bottle and immediately acidified overnight using 30% HCl (initial pH value: 7.56; final pH value: 1.9). Prior to ICP-OES analysis, the sample was filtered using a 0.45 µm membrane filter in order to remove impurities and matter in suspension. When necessary, the water samples were digested by UV treatment for 10 min.

3. RESULTS AND DISCUSSION

3.1. Electrochemical study of free 5-Br-PADAP and Fe(III) and Fe(II) complexes with 5-Br-PADAP

The electrochemical behavior of free 5-Br-PADAP in solution was first examined. Figure 1 shows the differential pulse voltammogram (DPV) recorded for 30 µM 5-Br-PADAP in 0.1 acetate buffer (pH 6.0) on Au electrode (red line).

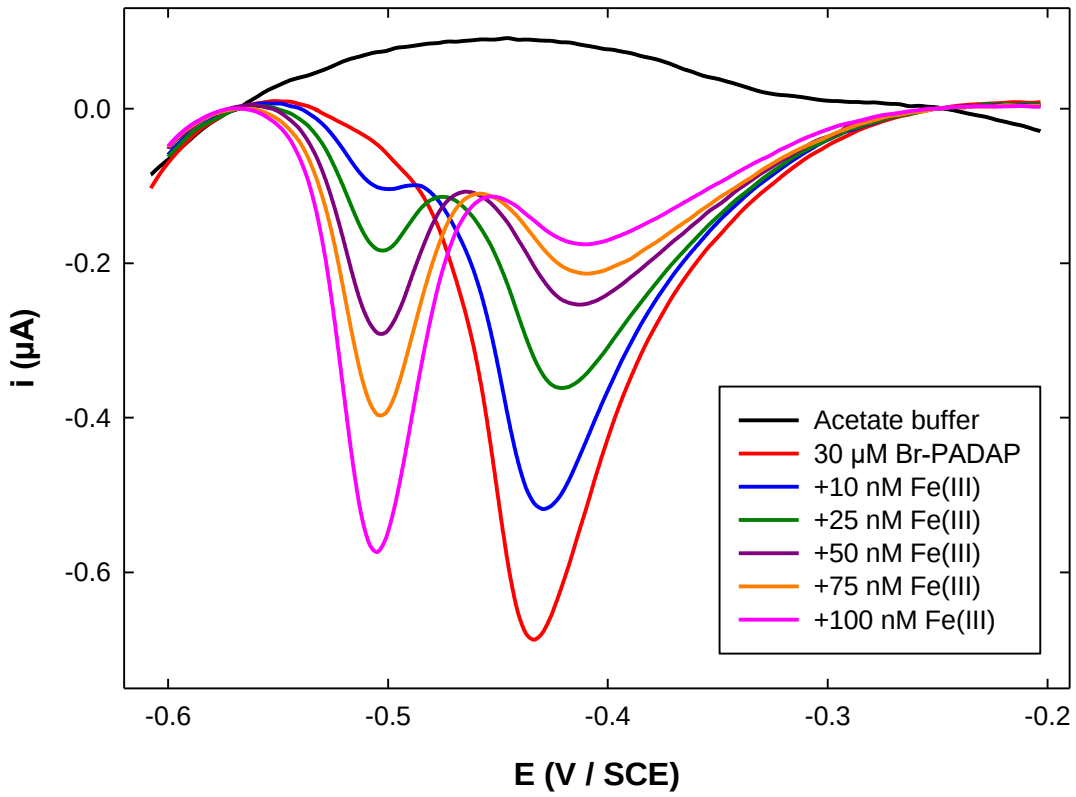

Figure 1. Differential Pulse Voltammograms recorded on Au electrode in 0.1 M acetate buffer (pH 6) (black line) containing 30 µM 5-Br-PADAP (red line) and increasing amounts of Fe(III) (other lines).

In order to mimic the experimental conditions used for Fe(III) determination and quantification, a preconcentration step (See Section 2.4.) was systematically applied before recording the DPV. The voltammogram exhibited a single reduction peak located at -0.43 V, which was attributed to 5-Br-PADAP reduction. This result including the peak potential value is in good agreement with the work by Zhu et al. who have reported a single reduction peak around -0.40 V for 5-Br-PADAP on both glassy carbon and reduced graphene oxide / gold nanoparticles modified electrodes [33], and in contradiction with another work from the same group in which no signal was observed despite of the presence of an excess 5-Br-PADAP [30]. The addition of 10 nM Fe(III) to the solution lead to the appearance of a small, second reduction peak located at -0.51 V together with a strong, unexpected decrease (around 25 %) in the peak current corresponding to 5-Br-PADAP reduction (Figure 1, blue line). The new peak at -0.51

V was assigned to the reduction of the Fe(III)/5-Br-PADAP complex, in accordance with several previous reports [30,33]. This latter complex was formed according to the following reaction:

$$M + n\ L \leftrightarrow ML_n \qquad \text{(Reaction 1)}$$

in which M stands for free Fe(III), L is 5-Br-PADAP and ML_n is the corresponding complex, n being the number of ligands coordinated to a metallic center. For the sake of clarity, the charges were omitted. It is worth noting that without the presence of 5-Br-PADAP in the solution, no signal was obtained on the DPV for a 10 nM Fe(III) concentration (not shown). Further addition of Fe(III) up to 100 nM induced an increase of the peak corresponding to the complex together with a decrease of the peak corresponding to free 5-Br-PADAP (Figure 1, green, violet, orange and pink lines). This behavior is consistent with a progressive complexation of Fe(III) by 5-Br-PADAP. However, it is noteworthy that while the increase in peak current for the complex and the decrease in peak current for free 5-Br-PADAP are in the same order of magnitude, the concentrations of Fe(III) and 5-Br-PADAP are actually not, this latter being at least in a 300-fold excess proportion. This observation clearly indicates that both reductions do not proceed via a similar pathway.

In order to clarify this result, complementary experiments were conducted by cyclic voltammetry using different scan rates. Figure 2A shows the evolution of 5-Br-PADAP reduction peak when scan rate was increased from 50 to 400 mV s^{-1}. The corresponding peak current increased with the increase in scan rate and the peak potential progressively shifted to more cathodic values from -0.51 to -0.61 V, in accordance with the irreversible character of the redox process. The peak current was found to be linearly dependent ($r^2 = 0.9826$) on the square root of the scan rate rather than on scan rate (Figures 2C and 2D, blue points), indicating that the reduction of 5-Br-PADAP is a mass transfer-controlled process. Similar experiments conducted on the Fe(III)/5-Br-PADAP complex (Figure 2B) showed that the corresponding peak current evolved in a linear trend ($r^2 = 0.9937$) as a function the square root of the scan rate (Figure 2C, red points), in accordance with another mass transfer-controlled redox process.

However, in this case, and contrary to what was observed for free 5-Br-PADAP, the plot of the peak current as a function of the scan rate (Figure 2D, red points) also exhibited a roughly linear trend ($r^2 = 0.9693$), suggesting that adsorption of the complex on the electrode surface plays a role in its reduction process. In order to quantify this latter contribution, the treatment recently reported by the group of Walcarius was applied here (not shown) [48]. Briefly, this method allows to evaluate the respective contribution of adsorption and diffusion to the overall current by plotting a normalized current as a function of the square root of the scan rate. In our case, it was found that adsorption contributed between 22 to 48 % of the recorded current, depending on the scan rate used. This result is in accordance with the need for a preconcentration step, which currently consists in an adsorption step, for the complex detection at low concentration. Thus, this combination of two different processes for the reduction of the Fe(III)/5-Br-PADAP complex, one limited by mass transfer in the solution and the other by adsorption onto the electrode surface may explain the similarity in the peak current values observed for the complex reduction and free 5-Br-PADAP reduction although the complex concentration was significantly lower, 5-Br-PADAP being assumed to be unaffected by the preconcentration step.

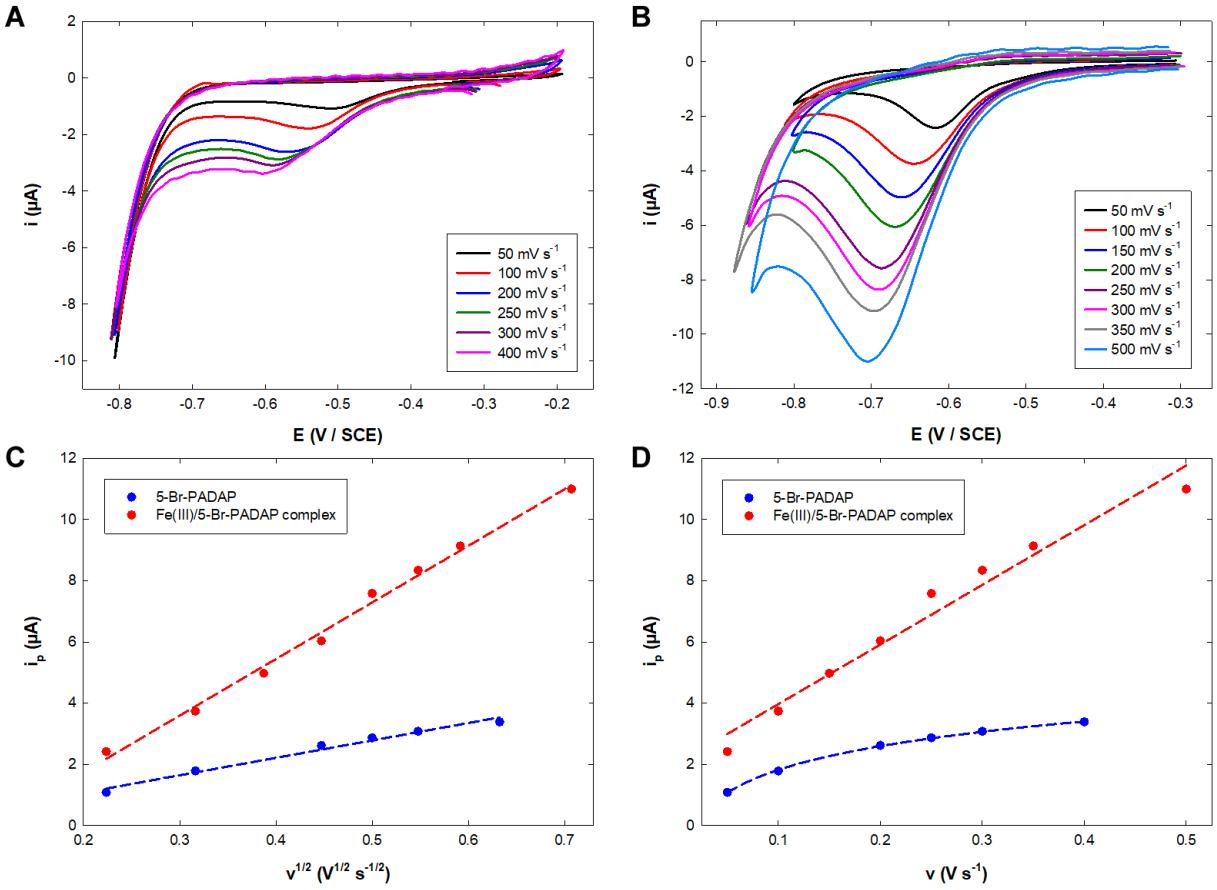

Figure 2. Cyclic voltammograms of (A) free 5-Br-PADAP and (B) Fe(III)/5-Br-PADAP complex recorded at different scan rates in 0.1 M acetate buffer (pH 6) on Au electrode. Evolution of the reduction peak current value of (blue) 5-Br-PADAP and (red) Fe(III)/5-Br-PADAP complex as a function of (C) square root of the scan rate and (D) scan rate.

Another complementary experiment was performed in order to understand the strong decrease in peak current for free 5-Br-PADAP when adding Fe(III): the same volumes of water were added to the 5-Br-PADAP-containing buffer solution, but without any Fe(III). A similar decrease in reduction peak current was noticed, although any complexation by Fe(III) could not be invoked (not shown). In fact, the decrease was due to the very poor solubility of 5-Br-PADAP in water, and subsequent progressive precipitation while adding water volumes, even if very small. This result probably explains why in the work by Zhu et al. [30] no reduction peak was observed for 5-Br-PADAP during Fe(III) detection, although the ligand was in large excess compared to metal ions.

3.2. Elucidation of the stoichiometry of the Fe(III)/5-Br-PADAP and Fe(II)/5-Br-PADAP complexes

The observation that 5-Br-PADAP reduction is a mass transfer-controlled process while Fe(III)/5-Br-PADAP complex reduction is limited both by diffusion and adsorption induces that a direct determination of the complex stoichiometry from the correlation of the amount of consumed ligand to the amount of added Fe(III), extracted from peak currents, would lead to an unrealistic value of the

metal:ligand ratio. Thus, in order to elucidate the stoichiometry of the Fe(III)/5-Br-PADAP complex, an alternative electrochemical experiment was conducted in which successive amounts of ligand were added to a fixed concentration of metal. For each amount a DPV was recorded using the same experimental conditions as before. Figure 3A shows the resulting voltammograms. As expected, an increasing peak located around -0.51 V was observed, which corresponds to the reduction of the Fe(III)/5-Br-PADAP complex formed according to Reaction 1.

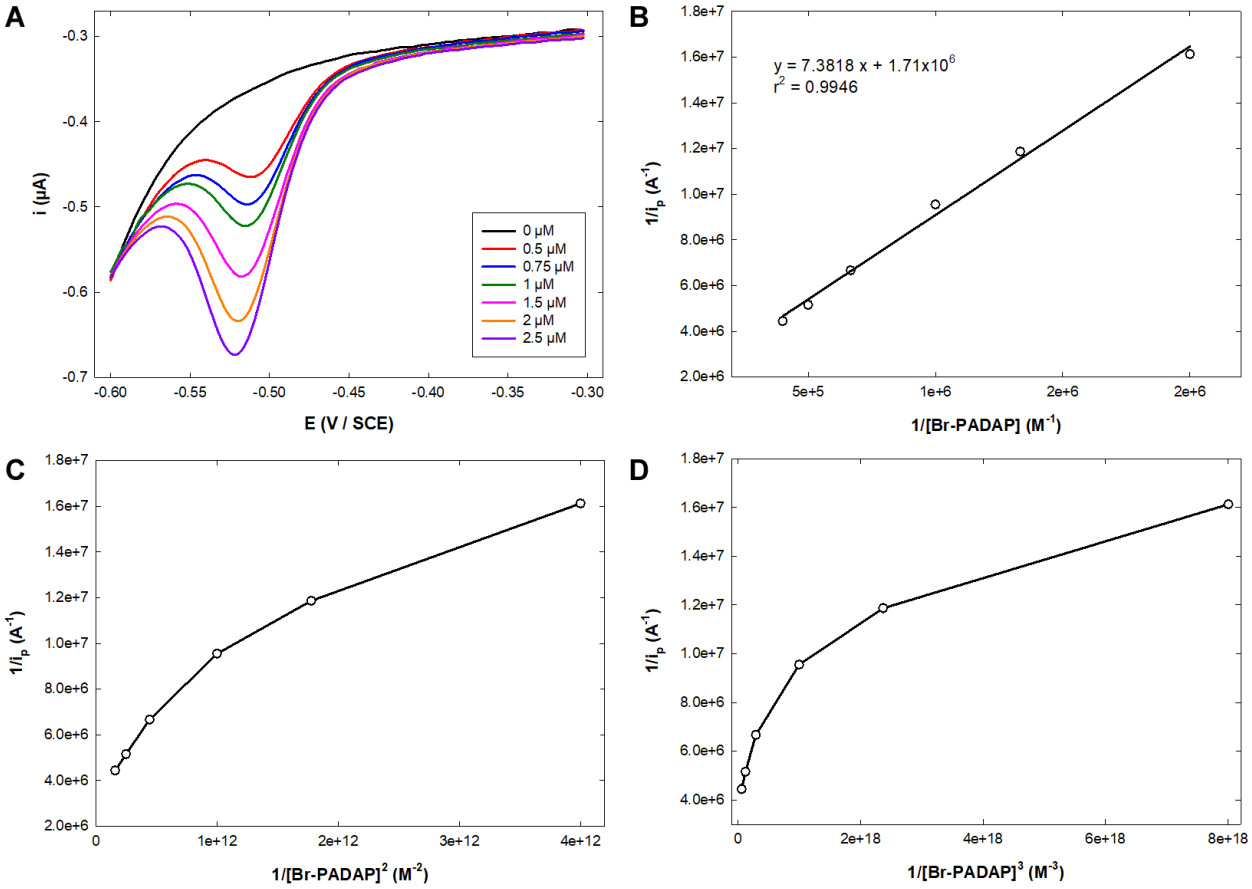

Figure 3. (A) Differential Pulse Voltammograms recorded on Au electrode in 0.1 M acetate buffer (pH 6) containing 2 µM Fe(III) and increasing amounts of 5-Br-PADAP. Plot of the inverse of the peak current corresponding to the reduction of the Fe(III)/5-Br-PADAP complex as a function of the inverse of 5-Br-PADAP concentration at the n power for (B) n = 1; (C) n = 2; (D) n = 3.

From this latter reaction, the stability constant β for the Fe(III)/5-Br-PADAP complex may be expressed as:

$$\beta = \frac{[ML_n]}{[M]\,[L]^n} \qquad (1)$$

Considering the adsorption process of the complex to be a key step in its electrochemical detection, Equation (1) can be adapted that way:

$$\beta = \frac{\Gamma_{ML_n}}{[M]\,[L]^n} \qquad (1')$$

in which Γ_{MLn} represents the surface concentration of the adsorbed complex on the electrode surface (mol cm^{-2}). If we define $\Gamma_{ML_n}^{total}$ as the complex surface concentration if all the metal cations present in solution have reacted with the ligands, the mass balance equation can be written:

$$V\,[M] = A\left(\Gamma_{ML_n}^{total} - \Gamma_{ML_n}\right) \quad (2)$$

Considering the reduction peak current to be proportional to the corresponding complex surface concentration, it is possible to write:

$$\frac{[M]}{\Gamma_{ML_n}} = \frac{A}{V}\left(\frac{i_{p,max} - i_p}{i_p}\right) \quad (3)$$

in which A is the electrode active surface area and V is the volume of the solution. This latter expression can be rearranged to express the ratio $i_{p,max}/i_p$:

$$\frac{i_{p,max}}{i_p} = \frac{V}{A}\left(1 + \frac{[M]}{\Gamma_{ML_n}}\right) \quad (4)$$

Identifying the concentration ratio using Equation (1'), the following expression is finally obtained:

$$\frac{1}{i_p} = \frac{V}{A}\left(\frac{1}{i_{p,max}} + \frac{1}{\beta\, i_{p,max}\,[L]^n}\right) \quad (5)$$

Figures 3B, 3C and 3D show the plot $1/i_p$ as a function of $1/[L]^n$ for n = 1, 2 and 3, respectively. From Equation (4), a linear plot is expected for the value of n which actually corresponds to the complex stoichiometry. Thus, this latter value was found to be n = 1, corresponding to a 1:1 Fe(III)/5-Br-PADAP ratio. This result is in accordance with the work by Zhao et Jin [31], who have used the same electrochemical method to get their result, but is in contradiction with the report by Oszwaldowski and Pikus [34], who have performed the determination of the stoichiometry using spectrophotometry and have found a 1:2 metal:ligand ratio. Using the regression equation from Figure 3B, it was possible to estimate the value of β from the intercept/slope ratio. A value $\beta = 2.3\times10^5$ was found, which suggests a much lower stability for the complex than that reported by Oszwaldowski and Pikus [34]. A similar treatment was applied to determine the stoichiometry of the Fe(II)/5-Br-PADAP complex, the oxidation of which appeared as a broad peak around 0.25 V (not shown). Using Equation (4) as for the Fe(III)/5-Br-PADAP complex, a 1:1 stoichiometry was found, together with a β value of 5.5×10^4. Once again, this suggests a much lower stability for the Fe(II)/5-Br-PADAP complex than that reported by Oszwaldowski and Pikus [34].

In order to get more information and definitely prove the Fe(III)/5-Br-PADAP and Fe(II)/5-Br-PADAP complexes stoichiometry, an alternative determination was performed using spectrophotometry, following the Bent-French method [35]. Briefly, this method consists in a logarithmic treatment of both Equation (1) and the Beer-Lambert law which allows to write the following expression:

$$\log A = \log \varepsilon + \log l + \log \beta + \log [M] + n \log [L] \quad (6)$$

in which A is the absorbance, ε the molar extinction coefficient of the complex and l the length of the UV-visible cell, according to the Beer-Lambert law, and β, n, [M] and [L] are the same as previously defined. Thus, the plot log A as a function of log [L] while maintaining [M] constant, allows the determination of n. Figure 4A shows the UV-visible spectra of both complexes in the range 400 –

850 nm. The shape of both spectra was comparable to that reported by Oszwaldowski and Pikus and typical for such kinds of azo chelates [34]. The Fe(III)/5-Br-PADAP and Fe(II)/5-Br-PADAP complexes exhibited a maximum in absorbance at 527 and 555 nm, respectively.

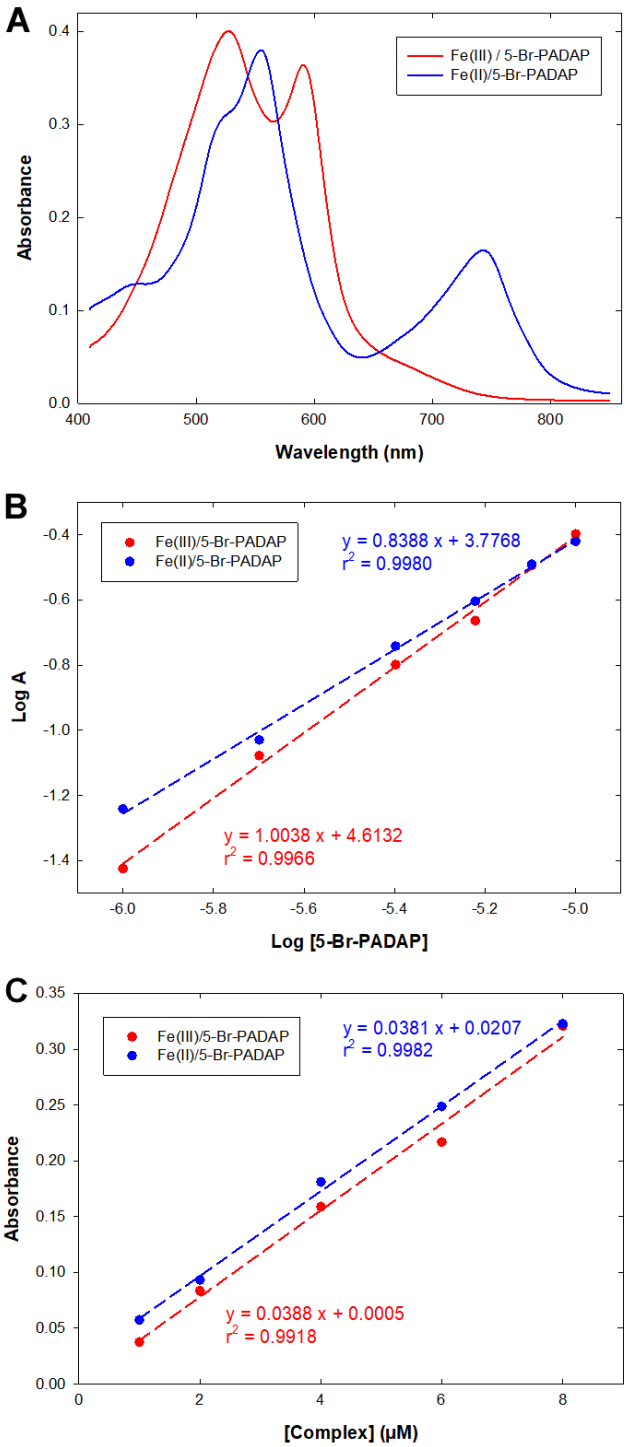

Figure 4. (A) UV-Visible spectra of the complexes Fe(III)/5-Br-PADAP and Fe(II)/5-Br-PADAP in a water/ethanol (4:1 volume) mixture; (B) Plot of the logarithm of the measured absorbance as a function of the logarithm of the concentration of added ligand for a 8 µM metal concentration; (C) Plot of the measured absorbance as a function of the complex concentration.

The value obtained for Fe(II)/5-Br-PADAP compared favorably to that found by Oszwaldowski and Pikus, but the value for Fe(III)/5-Br-PADAP (ca. 527 nm) was found to be significantly different. The reason for that could be the difference in the medium used for recording the spectra. The addition of successive amounts of 5-Br-PADAP in alcohol solution to a given, constant concentration of Fe(III) or Fe(II) in excess in aqueous solution induced an increase in absorbance due to the formation of the corresponding complexes. For both complexes the graph log A vs. log [L] was plotted (Figure 4B). In both cases, a linear relationship was obtained, the slope of which allowed the value of n to be extracted: this value was found to be 1.00 and 0.84 for Fe(III)/5-Br-PADAP and Fe(II)/5-Br-PADAP complexes, respectively, thus definitely confirming the 1:1 stoichiometry determined by DPV experiments. These results are in contradiction with the finding by Oszwaldowski and Pikus who have also used the Bent-French method and have reported a 1:2 stoichiometry for both complexes [34]. However, in the corresponding report the graphs log A vs. log [L] were not provided, so that it is difficult to further discuss on the observed discrepancy.

Finally, the graphs A vs. complex concentration were plotted for both complexes (Figure 4C). Both exhibited a linear trend, in accordance with the Beer-Lambert law. From the slope of the curves which provided the ε value and using Equation (5), it was possible to estimate the stability constant β for both complexes: this latter was found 1.3×10^5 and 2.0×10^4 for Fe(III)/5-Br-PADAP and Fe(II)/5-Br-PADAP complexes, respectively. It is worth noting that, in order to decrease the uncertainty on the ε values, the UV-Visible measurements were performed in such a way that the water:alcohol volume ratio remained constant during the whole experiments. All the data upon the stoichiometry and the stability constant are summarized in Table 1.

Table 1. Stoichiometry and stability constant for Fe(III)/5-Br-PADAP and Fe(II)/5-Br-PADAP complexes determined by both UV-Visible and electrochemical measurements.

		Fe(III)/5-Br-PADAP	Fe(II)/5-Br-PADAP
Stoichiometry	DPV	1:1	1:1
	UV-Vis.	1:1	1:1
Stability constant	DPV	2.3×10^5	5.5×10^4
	UV-Vis.	1.3×10^5	2.0×10^4

Both β values obtained by spectrophotometry compared well with that previously determined by using DPV. Whatever the method used, the Fe(III)/5-Br-PADAP complex was found to be one order of magnitude more stable than the corresponding Fe(II)/5-Br-PADAP complex. Considering that there is no obvious reason for the stoichiometry to change while changing the oxidation degree of the metallic center from Fe(III) to Fe(II), these latter can be unambiguously assigned to be 1:1 on the basis of four different experiments.

3.3. Fe(III) and Fe(II) electrochemical determination using 5-Br-PADAP

Acetate buffer solutions containing low amounts of Fe(III) and Fe(II) were measured by adsorptive DPV after addition of 30 µM 5-Br-PADAP. Figure 5A shows the resulting curves obtained in the case of increasing amounts of Fe(III). The typical signal for the reduction of the Fe(III)5-Br-PADAP located around -0.51 V was observed, the peak current of which increased linearly with Fe(III) concentration (Figure 5B).

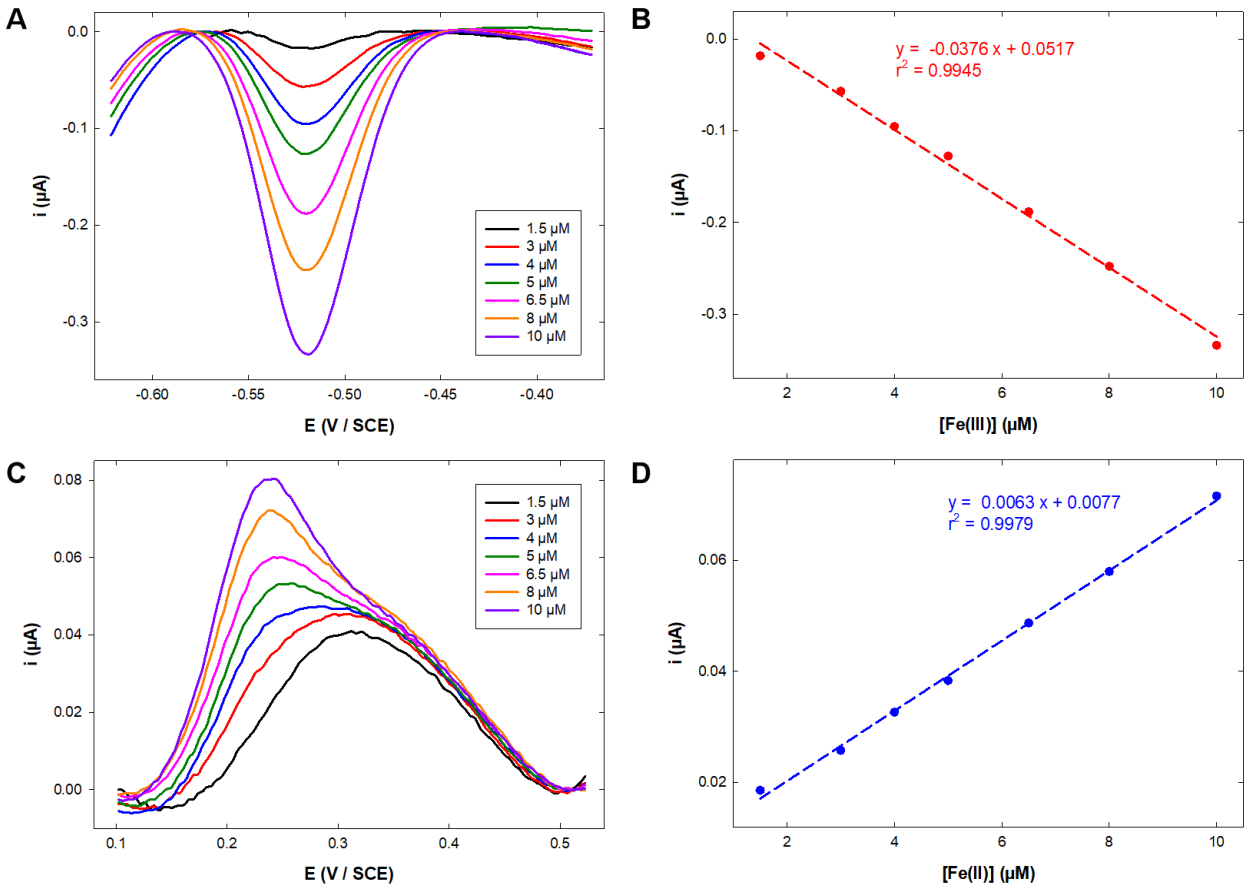

Figure 5. DPV recorded on Au electrode in 0.1 M acetate buffer (pH 6) containing 30 µM 5-Br-PADAP and increasing amounts of (A) Fe(III) and (C) Fe(II). Calibration plots obtained for (B) Fe(III) and (D) Fe(II).

The calibration plot exhibited a clear linear trend in the range 1 µM – 10 µM, with a sensitivity of 0.0376 µA μM^{-1}. This result suggests that, despite of the poor solubility of 5-Br-PADAP in water, the method can be used for the determination of Fe(III) in concentration ranges higher than that reported by Zhu et al., whose upper concentration limit was 1 µM [33]. The same experiment was conducted with increasing amounts of Fe(II). In this case, a broad anodic peak was noticed around 0.31 V for the lowest Fe(II) concentrations (Figure 5C). While increasing Fe(II) concentration, this latter peak progressively changed to a narrower peak with a more classical shape located at 0.25 V, associated to a post-peak

shoulder. These signals were assigned to the Fe(II)/5-Br-PADAP oxidation, despite of the change in peak morphology which remained unclear to us. The plot of the peak current as a function of Fe(II) concentration provided a linear calibration plot in the range 1 µM – 10 µM with a corresponding sensitivity of 0.0063 µA μM^{-1} (Figure 5D). It is worth noting that both of the recorded peak currents and the calculated sensitivity in the case of Fe(II) were much lower than that obtained in the case of Fe(III). All these results are summarized in Table 2 for the sake of comparison with literature data.

Table 2. Detection and quantification of Fe^{3+} and Fe^{2+} using complexation with 5-Br-PADAP.

Detection technique	Target	Stoichiometry (metal:ligand)	Linear range (µM)	LOD[a] (nM)	Ref.
Spectrophotometry	Fe^{3+}	1:2	up to 14	-	[36]
Spectrophotometry	Fe^{2+}	1:2	0.018 – 0.143	-	[38]
Spectrophotometry	Fe^{2+}	-	up to 11.6	-	[39]
Spectrophotometry	Fe^{2+}	1:2 *	0.358 – 8.95	322	[34]
	Fe^{3+}	1:2 *	0.358 – 8.95	322	
Spectrophotometry	Fe^{2+}	1:2	0.0895 – 2	14.3	[40]
Spectrophotometry	Fe^{2+}	-	0.0895 – 7.2	26.9	[32]
Spectrophotometry	Fe^{2+}	1:1	-	71.6	[41]
Spectrophotometry	Fe^{2+}	1:2	6.45 – 89.5	1970	[42]
Spectrophotometry	Fe^{2+}	1:2	-	610	[43]
Spectrophotometry[b]	Fe^{2+}	1:2	-	53.7	[44]
Spectrophotometry[c]	Fe^{3+}	-	0.358 – 89.5	179	[45]
Adsorptive LSV[d]	Fe^{3+}	1:1 *	0.00025 – 0.1	-	[31]
Derivative adsorption chronopotentiometry	Fe^{3+}	1:1	0.0067 – 0.17	2	[46]
Derivative adsorption chronopotentiometry	Fe^{3+}	1:1	-	-	[47]
SW[e] adsorptive cathodic stripping voltammetry	Fe^{3+}	?	0.00555 – 0.448	1.67	[37]
DP[f] adsorptive cathodic stripping voltammetry	Fe^{3+}	?	0.03 – 3	3.5	[33]
DP[f] adsorptive cathodic stripping voltammetry	Fe^{3+}	1:2	0.01 – 1	1.2	[30]
DP[f] adsorptive cathodic stripping voltammetry	Fe^{2+}	1:1 *	1 – 10	-	This
	Fe^{3+}	1:1 *			work

[a] Limit of detection; [b] Second derivative spectrophotometry; [c] Third derivative spectrophotometry; [d] linear sweep voltammetry; [e] square wave voltammetry; [f] differential pulse voltammetry; * works in which a determination of the stoichiometry has been conducted.

3.4. Analysis of a natural water sample

Tests were conducted on a natural water sample from the Canal du Midi collected on the campus of the university. After addition of concentrated HCl and stirring overnight, 25 mL of the sample were analyzed using the established procedure. With respect to Fe(III) determination, after addition of 30 µM 5-Br-PADAP a well-defined reduction peak at -0.49 V was observed together with a small, broad

shoulder located around -0.40 V (not shown). The peak at -0.49 V was unambiguously assigned to the reduction of the Fe(III)/5-Br-PADAP complex on the basis of our previous observations. The shoulder was not attributed to any reduction of a species, since the natural sample was not treated, except acidification for conditioning purpose. Three successive amounts of Fe(III) were then spiked into the natural water sample, and the corresponding DPV were recorded, allowing a regression graph to be plotted (Figure 6A, full red points). From the equation of the plot, a concentration [Fe(III)] = 1.3 µM was obtained for the natural water sample.

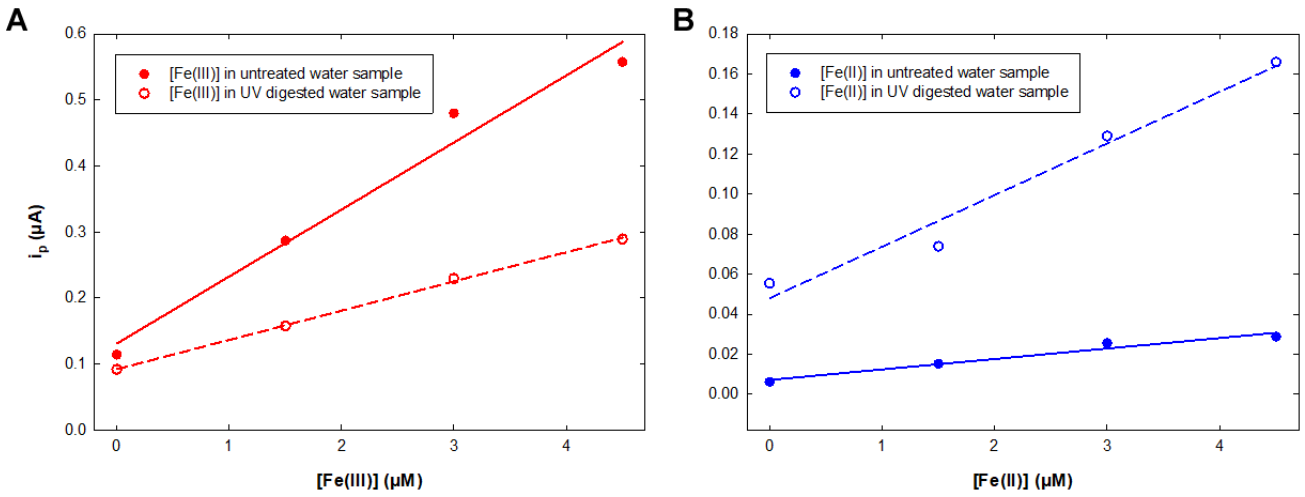

Figure 6. Regression plots obtained for three successive spike concentrations of (A) Fe(III) and (B) Fe(II) in (full color points) untreated or (empty color points) UV-digested natural water samples from Canal du Midi.

A similar procedure was used for the determination of Fe(II): in this latter case, an oxidation peak located at 0.23 V was observed, and spiking three successive amounts of Fe(II) allowed to extract a concentration [Fe(II)] = 1.4 µM (Figure 6B, full blue points). These values were compared to that obtained using the reference analysis technique, namely inductive coupled plasma - optical emission spectroscopy (ICP-OES) which provided a value for total Fe [^{t}Fe] = 4.5 µM. Thus, only 60 % of ^{t}Fe was recovered using the voltammetric analysis via 5-Br-PADAP complexation. This result suggested that 5-Br-PADAP is actually not a complexing agent strong enough to catch Fe(III) and Fe(II) from its corresponding complexes with organic matter. In order to support this hypothesis, the same analyses were conducted on a water sample from the Canal du Midi after organic matter UV digestion. The corresponding responses obtained after three successive spikes of Fe(III) and Fe(II) are depicted on Figure 6A and 6B (empty red and blue points, respectively). The corresponding values for Fe(III) and Fe(II) concentrations are summarized in Table 3. In this latter cases, values of 2.3 µM and 1.7 µM were found for Fe(III) and Fe(II) concentration, respectively. In accordance with the hypothesis of a strong complexation of Fe(III) and Fe(II) with organic matter, both concentration values were found to be higher than that obtained when the natural water sample did not experience any treatment for organic matter digestion. However, still only 89 % of ^{t}Fe was recovered, ca. 4.0 µM. This latter result can be

accounted for considering the values found in this work for the β values of Fe(III)/5-Br-PADAP and Fe(II)/5-Br-PADAP complexes, which suggest the existence of an equilibrium between free and complexed Fe(III) or Fe(II) species, and the subsequent detection of only a part of the present species.

Table 3. Fe speciation in untreated and UV-digested natural water samples from canal du Midi.

UV digestion	Fe(II) (µM)[a]	Fe(III) (µM)[a]	^{t}Fe (µM)[b]
No	1.4	1.3	2.7 (60%)[c]
Yes	1.7	2.3	4 (89%)

[a] Determined by electrochemistry.

[b] [^{t}Fe] = [Fe(III)] + [Fe(II)].

[c] The percentage of recovery was calculated from the ratio [Fe(III)] + [Fe(II)] / [^{t}Fe], the latter concentration being obtained by ICP-OES.

4. CONCLUSIONS

In this work, the stoichiometry of the complexes formed between Fe(III) and Fe(II) with 5-Br-PADAP was definitely proved to be 1:1. On the basis of both electrochemical and spectrophotometric studies, the 4 different converging determinations that were conducted give a statistical power to this result. Contrary to free 5-Br-PADAP the reduction of which was proved to be a mass transfer-limited process, the reduction of the Fe(III)/5-Br-PADAP complex was found to be dependent on both diffusion and adsorption phenomena, thus highlighting the role of the preconcentration step in low Fe(III) determination in the presence of 5-Br-PADAP. The Fe(III)/5-Br-PADAP complex was found to be one order of magnitude more stable than the corresponding Fe(II) complex. The method using 5-Br-PADAP complexation and subsequent preconcentration by adsorption on the electrode surface was demonstrated to be efficient in the 1 – 10 µM concentration range for both Fe(III) and Fe(II). Tests in natural water samples from Canal du Midi showed that without pretreatment of the sample only Fe(III) and Fe(II) from the most labile complexes with organic matter can be determined, since 5-Br-PADAP is a complexing agent not strong enough to catch Fe(III) or Fe(II) from these latter. In order to access more reliable values for Fe(III) and Fe(II), a UV treatment of the sample appeared to be mandatory step.

References

1. K. H. Wedepohl, *Geochim. Cosmochim. Acta*, 59 (1995) 1217.
2. S. R. Taylor and S. M. McLennan, *The continental crust: Its composition and evolution,* London (1985).
3. P. T. Lieu, M. Heiskala, P. A. Peterson and Y. Yang, *Mol. Aspects Med.*, 22 (2001) 1.
4. M. E. Conrad, J. M. Umbreit and E. G. Moore, *Am. J. Med. Sci.*, 318 (1999) 213.
5. T. Dandekar and M. W. Hentze, *Trends Genet.*, 11 (1995) 45.
6. M. Miethke and M. A. Marahiel, *Microbiol. Mol. Biol. Rev.*, 71 (2007) 413.
7. J. H. Martin and S. E. Fitzwater, *Nature (London)*, 331 (1988) 341.
8. J. H. Martin and R. M. Gordon, *Deep-Sea Res., Part A.*, 35 (1988) 177.
9. P. Ugo, L. M. Moretto, D. Rudello, E. Birriel and J. Chevalet, *Electroanalysis*, 13 (2001) 661.

10. J. H. T. Luong, E. Lamb and K. B. Male, *Anal. Methods*, 6 (2014) 6157.
11. J. H. Martin, R. M. Gordon, S. E. Fitzwater and W. W. Broenkow, *Deep-Sea Res., Part A.*, 36 (1989) 649.
12. J. W. Munger, J. M. Waldman, D. J. Jacob and M. R. Hoffmann, *J. Geophys. Res. Oceans*, 88 (1983) 5109.
13. D. B. Johnson, *Water, Air, Soil Pollut. Focus*, 3 (2003) 47.
14. C. M. G. van den Berg, M. Nimmo, O. Abollino and E. Mentasti, *Electroanalysis*, 3 (1991) 477.
15. M. Lu, N. V. Rees, A. S. Kabakaev and R. G. Compton, *Electroanalysis*, 24 (2012) 1693.
16. A. Kot and J. Namiesńik, *TrAC, Trends Anal. Chem.*, 19 (2000) 69.
17. X. Liu and F. J. Millero, *Mar. Chem.*, 77 (2002) 43.
18. S. Pehkonen, *Analyst (Cambridge UK)*, 120 (1995) 2655.
19. M. Lin, X. Hu, D. Pan and H. Han, *Talanta*, 188 (2018) 135.
20. L. M. Laglera and D. Monticelli, *Curr. Opin. Electrochem.*, 3 (2017) 123.
21. M. Gledhill and C. M. G. van den Berg, *Mar. Chem.*, 47 (1994) 41.
22. A. P. Aldrich and C. M. G. van den Berg, *Electroanalysis*, 10 (1998) 369.
23. T. Nagai, A. Imai, K. Matsushige, K. Yokoi and T. Fukushima, *Limnology*, 5 (2004) 77.
24. R. Segura, M. I. Toral and V. Arancibia, *Talanta*, 75 (2008) 973.
25. J. Gun, P. Salaun and C. M. G. van den Berg, *Anal. Chim. Acta*, 571 (2006) 86.
26. C. M. G. van den Berg, *Anal. Chem.*, 78 (2006) 156.
27. L. M. Laglera, J. Santos-Echeandia, S. Caprara and D. Monticelli, *Anal. Chem.*, 85 (2013) 2486.
28. E. L. Rue and K. W. Bruland, *Mar. Chem.*, 50 (1995) 117.
29. P. L. Croot and M. Johansson, *Electroanalysis*, 12 (2000) 565.
30. Y. Zhu, X. Hu, D. Pan, H. Han, M. Lin, Y. Lu, C. Wang and R. Zhu, *Sci. Rep.*, 8:2576 (2018)
31. J. Zhao and W. Jin, *J. Electroanal. Chem.*, 267 (1989) 271.
32. B. Peng, Y. Shen, Z. Gao, M. Zhou, Y. Ma and S. Zhao, *Food Chem.*, 176 (2015) 288.
33. Y. Zhu, D. Pan, X. Hu, H. Han, M. Lin and C. Wang, *Sensors Actuators B: Chem.*, 243 (2017) 1.
34. S. Oszwaldowski and A. Pikus, *Talanta*, 58 (2002) 773.
35. H. E. Bent and C. L. French, *J. Am. Chem. Soc.*, 63 (1941) 568.
36. W. Fu-sheng, Z. Yu-rui and Y. Fang, *Anal. Lett.*, 14 (1981) 241.
37. E. M. Ghoneim, *Talanta*, 82 (2010) 646.
38. M. Vitouchova, L. Jancar and L. Sommer, *Fresenius J. Anal. Chem.*, 343 (1992) 274.
39. A. C. S. Costa, S. L. C. Ferreira, M. G. M. Andrade and I. P. Lobo, *Talanta*, 40 (1993) 1267.
40. H. Filik and D. Giray, *Food Chem.*, 130 (2012) 209.
41. A. Flavia de Oliveira e Silva, W. Victor de Castro and F. Pereira de Andrade, *Food Chem.*, 242 (2018) 205.
42. P. Phansi, K. Danchana, S. L. C. Ferreira and V. Cerda, *Food Chem.*, 277 (2019) 261.
43. C. Andreu, K. Danchana and V. Cerda, *Anal. Lett.*, 53 (2020) 2775.
44. K. Sozgen, Esma, *Talanta*, 62 (2004) 971.
45. M. A. Taher and B. K. Puri, *Talanta*, 43 (1996) 247.
46. W. Jin and J. Wang, *Anal. Chim. Acta*, 245 (1991) 77.
47. W. Jin and K. Liu, *Anal. Chim. Acta*, 347 (1997) 257.
48. D. Basnig, N. Vilá, G. Herzog and A. Walcarius, *J. Electroanal. Chem.*, 872 (2020) 113993.